Degradation Process of Lead Chromate in Paintings by Vincent van Gogh Studied by Means of Spectromicroscopic Methods. 4. Artificial Aging of Model Samples of Co-Precipitates of Lea...

ARTICLE *in* ANALYTICAL CHEMISTRY · JANUARY 2013

Impact Factor: 5.64 · DOI: 10.1021/ac3021592 · Source: PubMed

8 AUTHORS, INCLUDING:

Koen Janssens
University of Antwerp
381 PUBLICATIONS **5,185** CITATIONS
SEE PROFILE

Costanza Miliani
Italian National Research Council
135 PUBLICATIONS **2,077** CITATIONS
SEE PROFILE

Bruno Brunetti
Università degli Studi di Perugia
178 PUBLICATIONS **2,432** CITATIONS
SEE PROFILE

Mariangela Cestelli Guidi
INFN - Istituto Nazionale di Fisica Nucleare
119 PUBLICATIONS **816** CITATIONS
SEE PROFILE

analytical chemistry

Article

pubs.acs.org/ac

Degradation Process of Lead Chromate in Paintings by Vincent van Gogh Studied by Means of Spectromicroscopic Methods. 4. Artificial Aging of Model Samples of Co-Precipitates of Lead Chromate and Lead Sulfate

Letizia Monico,[†,‡] Koen Janssens,[*,‡] Costanza Miliani,[§] Geert Van der Snickt,[‡] Brunetto Giovanni Brunetti,[†,§] Mariangela Cestelli Guidi,[∥] Marie Radepont,[‡,⊥] and Marine Cotte[⊥,@]

[†]Centre SMAArt and Dipartimento di Chimica, Università degli Studi di Perugia, via Elce di Sotto 8, I-06123 Perugia, Italy

[‡]Department of Chemistry, University of Antwerp, Groenenborgerlaan 171, B-2020 Antwerp, Belgium

[§]Istituto CNR di Scienze e Tecnologie Molecolari (CNR-ISTM), c/o Dipartimento di Chimica, Università degli Studi di Perugia, via Elce di Sotto 8, I-06123 Perugia, Italy

[∥]INFN - Laboratori Nazionali di Frascati, Via E. Fermi 40, I-00044 Frascati (Roma), Italy

[⊥]Laboratoire d'Archéologie Moléculaire et Structurale, CNRS UMR8220, 3, rue Galilée, F-94200 Ivry-Sur-Seine, France

[@]European Synchrotron Radiation Facility (ESRF), 6, rue Jules Horowitz, F-38000 Grenoble, France

Supporting Information

ABSTRACT: Previous investigations about the darkening of chrome yellow pigments revealed that this form of alteration is attributable to a reduction of the original Cr(VI) to Cr(III), and that the presence of sulfur-containing compounds, most often sulfates, plays a key role during this process. We recently demonstrated that different crystal forms of chrome yellow pigments ($PbCrO_4$ and $PbCr_{1-x}S_xO_4$) are present in paintings by Vincent van Gogh. In the present work, we show how both the chemical composition and the crystalline structure of lead chromate-based pigments influence their stability. For this purpose, oil model samples made with in-house synthesized powders of $PbCrO_4$ and $PbCr_{1-x}S_xO_4$ were artificially aged and characterized. We observed a profound darkening only for those paint models made with $PbCr_{1-x}S_xO_4$, rich in SO_4^{2-} ($x \geq 0.4$), and orthorhombic phases (>30 wt %). Cr and S K-edge micro X-ray absorption near edge structure investigations revealed in an unequivocal manner the formation of up to about 60% of Cr(III)-species in the outer layer of the most altered samples; conversely, independent of the paint models' chemical composition, no change in the S-oxidation state was observed. Analyses employing UV−visible diffuse reflectance and Fourier transform infrared spectroscopy were performed on unaged and aged model samples in order to obtain additional information on the physicochemical changes induced by the aging treatment.

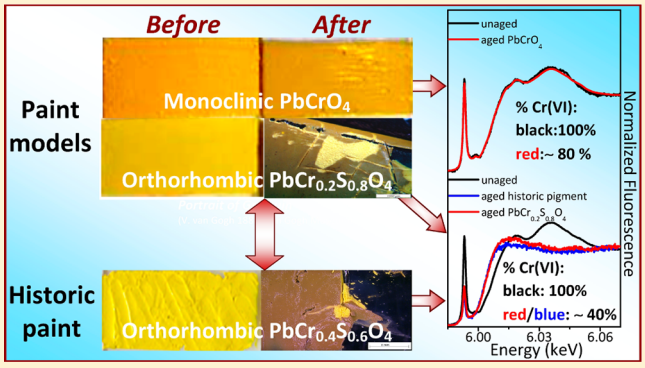

In recent years, spectroscopic investigations on paintings from ancient to modern times have yielded valuable information both on the type of pigments present and on the mechanisms of their alteration. The combined use of conventional spectroscopic techniques makes the characterization of artists' palettes possible.[1−4] More advanced methods based on synchrotron radiation (SR) X-rays have permitted the alteration mechanism of pigments such as vermillion,[5,6] Prussian blue,[7] smalt,[8] and cadmium yellow[9,10] to be elucidated. There is also a growing interest in the use of noninvasive methods for in situ elemental [such as X-ray fluorescence (XRF)] and molecular spectroscopic analysis (such as near- and mid-FTIR and Raman) in view of their capability to yield information about the pigments' identification by noncontact examination of the entire work of art.[11]

Commonly used by Van Gogh and his contemporaries, chrome yellow pigments have been extensively studied in recent years, because of their low photochemical and environmental stability.[12,13] In the first two parts of this series of papers,[12,13] the alteration mechanism of these compounds was attributed to a reduction of the original Cr(VI) to Cr(III), while in part 3,[14] we have demonstrated that different chrome yellow types [$PbCrO_4$ and $PbCr_{1-x}S_xO_4$ (where $0 < x < 1$)] have been effectively used by Van Gogh.

Received: July 14, 2012
Accepted: October 10, 2012
Published: October 10, 2012

In what follows, we explore the susceptibility of these different forms of chrome yellow toward darkening under different artificial aging conditions, and we describe our attempts to reproduce the alteration process of paint models based on $PbCr_{1-x}S_xO_4$ solid solutions and mixtures thereof that are similar to those used by artists of the 19th and 20th centuries.

Considering the capability of SR X-ray techniques to visualize, with high spatial resolution and corresponding sensitivity, the distribution of specific Cr- and S-species, micro-X-ray absorption near edge structure (μ-XANES) analyses at the Cr and S K-edges were performed on chrome yellow model samples before and after photochemical aging. Supporting analytical methods, such as UV−visible diffuse reflectance and Fourier transform infrared (FTIR) spectroscopy, were employed to obtain additional information associated with the darkening of paints.

It was found that a profound darkening is present only for those paint models made of $PbCr_{1-x}S_xO_4$, rich in SO_4^{2-} ($x \geq 0.4$) and orthorhombic phases (>30 wt %).

EXPERIMENTAL SECTION

Synthesis of $PbCrO_4$ and $PbCr_{1-x}S_xO_4$ and Preparation of Paint Models. Powders of $PbCrO_4$ (S^*_{1mono} and S^*_{1ortho}) and $PbCr_{1-x}S_xO_4$ (S^*_{3A}, S^*_{3B}, S^*_{3C}, and S^*_{3D}) were synthesized as described in part 3 of this series of papers.[14] A list of these in-house synthesized compounds and some of their properties are reported in Table 1 (see reference 14 for further details).

Table 1. List and Composition of In-House Synthesized/Commercial Lead Chromate-Based Powders (S^*_{1mono}, S^*_{3A}−S^*_{3D}, and D^*_1) and Unaged Historic Chrome Yellow Paint A[a]

	x-ray diffraction		
sample[b]	phases		mass fraction (%)
S^*_{1mono}	$PbCrO_4$	monoclinic	98.82(5)
		orthorhombic	1.18(6)
S^*_{3A}	$PbCr_{0.89}S_{0.11}O_4$	monoclinic	100
S^*_{3B}	$PbCr_{0.76}S_{0.24}O_4$	monoclinic	100
S^*_{3C}	$PbCr_{0.4}S_{0.6}O_4$	monoclinic	60.0(2)
		orthorhombic	31.1(1)
	$PbCrO_4$	orthorhombic	9.10(8)
S^*_{3D}	$PbCr_{0.2}S_{0.8}O_4$	monoclinic	11.5(3)
		orthorhombic	74.7(3)
	$PbCrO_4$	orthorhombic	13.8(2)
D^*_1	$PbCr_{0.52}S_{0.48}O_4$	monoclinic	75.0(1)
	$PbSO_4$	orthorhombic	25.0(1)
A	$PbCr_{0.4}S_{0.6}O_4$	orthorhombic	41.0(1)
		orthorhombic	58.0(1)
		monoclinic	1.0 (1.0)

[a]See 14 for further details. [b]The XRD pattern of S^*_{1ortho} resembles that reported in literature.[14]

The * indicates the pure inorganic powders not yet mixed with a binding medium. Paint models (S_1−S_{3D}) were prepared by mixing these powders with linseed oil in a 4:1 pigment:oil mass ratio and application of the mixture on polycarbonate microscopy slides. Employing the same mass ratio, paint model D_2 was prepared by mixing pure $PbCrO_4$ and pure $PbSO_4$ powders (both Aldrich) in a 1:2 molar ratio, while sample D_1 was prepared using a commercially available $PbCr_{1-x}S_xO_4$ powder (CIBA and BASF). In order to evaluate the consequences of the additional presence of sulfate/sulfide species not incorporated inside the crystalline structure, oil paint models S_{1Ba} and S_{1Zn} were prepared by mixing S^*_{1mono} with ca. 1% $BaSO_4$ (Fluka) or ZnS (Aldrich), while samples S_{3CBa} and S_{3CZn} were obtained by adding similar amounts of the same compounds to S^*_{3C}.

Photochemical Accelerated Aging. *UVA-visible Light Exposure.* All paint models have been aged for 800 h, employing a SOLARBOX 1500e system (CO.FO.ME.GRA., Milano, Italy). This chamber is equipped with a xenon lamp (550 W/m^2) emitting between 290 and 800 nm (UVA-visible light) and operating at a temperature between 50 and 60 °C. A soda-lime glass UV filter between the light source and the samples allows simulating exposure to indoor light conditions.

Irradiation with Different Wavelength Bands of the UV−visible Light. Historical paint A was obtained from a paint tube used by a late 19th century artist; this bright yellow material shows a profound darkening upon artificial aging.[12] In view of the similarities between historic paint A and the S_{3D} material, both with respect to their chemical composition (SO_4^{2-} > wt 50%) and crystal structure (mainly orthorhombic $PbCr_{1-x}S_xO_4$), photochemical aging using various wavelength ranges was performed on paint coupons with S_{3D} composition. The final aim was to investigate any analogy between the response of samples A and S_{3D} to light exposure and to evaluate the influence of specific wavelength ranges on the degradation process.

Several paint coupons of S_{3D} were exposed for 98 h to the light produced by a 175 W Cermax xenon lamp; this emits a high intensity and focused light between 200 and 1100 nm. For the aging of S_{3D} coupons, appropriate filters (refer to Figure S-1A of the Supporting Information to see the corresponding spectral irradiance of the lamp and UV−visible transmission spectra of the filters) were used to select the following wavelength ranges of the UV−visible spectrum: "UVA-vis" ($\lambda \geq 300$ nm, soda-lime glass filter), "UV" ($240 \leq \lambda \leq 400$ nm, model UG 11, Schott AG), "blue" ($335 \leq \lambda \leq 525$ nm, model CS 5-60-5543, Kopp Glass) and "red" ($\lambda \geq 570$ nm, model 51311, Oriel). By employing the same aging protocol, the treatment of an additional S_{1ortho} paint was carried out only by UVA-vis light.

A water filter was used during each experiment, except for those in which a soda-lime glass filter was employed. In the presence of the water filter, the measured temperature close to the sample was around 45−50 °C, while in absence of this device it was 30 °C.

Analytical Methods. *UV−visible.* A JASCO V-570 spectrophotometer was employed. Diffuse reflectance spectral data were recorded between 200 and 1000 nm, using a 5 and 20 nm spectral bandwidth in the UV−visible and NIR region, respectively. The acquisition of an unsaturated spectrum from a pellet of unaged S^*_{3D} powder (Figure S-1B of the Supporting Information), prepared by diluting the pigment 30:1 with $BaSO_4$, was necessary to select the optical filters to be used during the aging at different wavelength bands of the UV−visible light.

Colorimetry. A portable in-house built prototype spectrophotometer,[15] equipped with an integrating sphere with a 6 mm diameter viewing aperture and a fiber-optic system, was used. Software, interfaced with the instrument, converts the reflectance spectra into CIE L*a*b* chromatic coordinates under the CIE illuminant D65 and 10° angle observer. Between 3 and 5 measurements were collected for each sample, with an

dx.doi.org/10.1021/ac3021592 | Anal. Chem. 2013, 85, 860−867

exposure time of 300 ms and average values of the chromatic coordinates L^*, a^*, and b^* determined. The total color changes were expressed in terms of $\Delta E^* = (\Delta L^{*2} + \Delta a^{*2} + \Delta b^{*2})^{1/2}$.

Transmission and Micro-Attenuated Total Reflection (μ-ATR) Mid-FTIR. Analyses were performed employing a JASCO IMV-4000 interfaced with an FTIR 4100 spectrometer. Transmission data were acquired in the range of 4000−400 cm^{-1}, at a 2 cm^{-1} resolution, using 100 scans. Analyses in the ATR mode were performed using an objective (30×) equipped with a diamond internal reflection element (model ATR-30-D, JASCO), in the range of 6000−600 cm^{-1}, at a 4 cm^{-1} resolution, using 1000 scans.

ATR Far-FTIR. A Vertex 70 V spectrometer (Bruker Optics) was used. Spectra were acquired under vacuum (final pressure < 0.2 mbar) by an ATR-diamond crystal, in the range of 1500−150 cm^{-1}, at 4 a cm^{-1} resolution, using 64 scans.

Portable Mid-FTIR. Pseudoabsorption spectra (reflection mode) were collected by a compact ALPHA Bruker Optics spectrometer from spots of ca. 5 mm in diameter, in the energy range of 6000−375 cm^{-1}, at a 4 cm^{-1} resolution, using 100 scans.

SR μ-XANES. Samples were analyzed at the ID21 beamline of ESRF (Grenoble, France). Spectra were acquired in the XRF mode by scanning the primary energy both around the Cr K-edge (5.96−6.09 keV) and the S K-edge (2.46−2.53 keV) with energy steps of 0.2 and 0.18 eV, respectively. Investigations under vacuum (10^{-6} mbar) in the unfocused mode (collimated beam, 0.2 mm diameter) were performed at these edges; measurements by a focused X-ray beam [0.7 × 0.2 μm^2 diameter (hxv)] were carried out at the Cr K-edge. A metallic Cr foil and a $CaSO_4 \cdot 2H_2O$ reference powder were used for energy calibration. Contributions from S and Pb were separated by the PyMca software.[16]

ATHENA[17] was employed to perform a linear combinatorial fitting of the XANES spectra of unknown mixtures of Cr species against a library of XANES spectra of Cr reference compounds.

RESULTS AND DISCUSSION

Reproduction of the Darkening Process of Historic Paint A. After treatment by UVA-Vis light, S_{3D} features the formation of a thin brown superficial layer (Figure 1A, optical microscopy images captured on the surface, OM_1, and on a cross section, OM_2) that is similar to the one previously observed on aged sample A.[12]

Color changes observed with the naked eye (Figure 1A) are confirmed in a more quantitative manner by UV−visible diffuse reflectance spectroscopy, through the formation of a new band between 530 and 620 nm on spectra of aged paints S_{3D} and A (Figure 1B).

Colorimetric measurements (Figure S-2 of the Supporting Information) show that a significant decrease both in L^* (luminance) and b^* values (yellow component) are responsible for the total observed color change ΔE^*, whereas the difference in a^* values (red component) were small/negligible.

In Figure 1C, ΔE^* values recorded during the exposure of S_{3D} paints to different wavelength bands are compared versus aging time. This material visibly aged under the influence of either UV or blue light, but not as quickly as under the UVA-Vis conditions. In terms of color changes, the same evolution was observed (cf. Figure S-2 of the Supporting Information). No color change and differences in the UV−visible spectrum were observed when S_{3D} was irradiated by red light. As reported

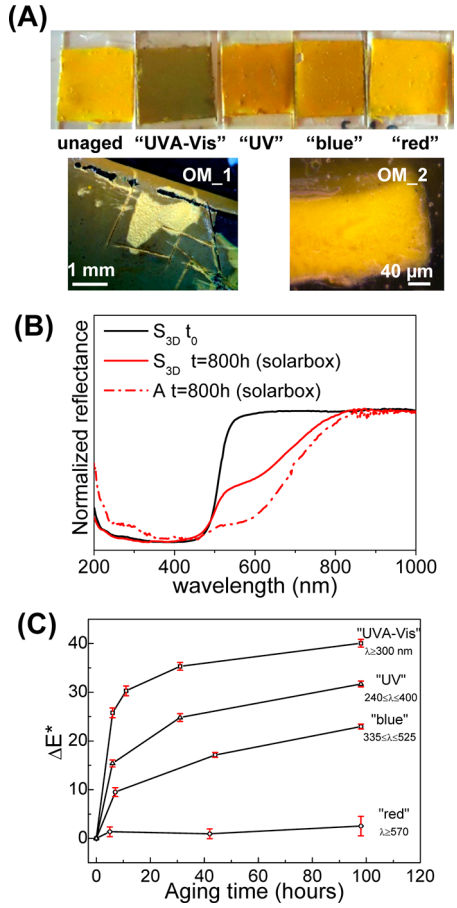

Figure 1. (A) (top) Photographs of S_{3D} paints ($PbCr_{0.2}S_{0.8}O_4$) aged by different UV−visible wavelength bands and (bottom) visible light microscopy images of unembedded (OM_1) and embedded (OM_2) UVA-Vis-aged S_{3D}. (B) UV−visible diffuse reflectance spectra of S_{3D} and A paints (black) before and (red) after light exposure (Solarbox, 800 h). (C) Change of ΔE^* during exposure to different photochemical aging treatments of S_{3D} vs the aging time.

by Cole,[18] the graphs of Figure 1C demonstrate that the darkening of the pigment is very fast during the first hours of the irradiation and then continues more slowly.

After aging, the transmission mid-FTIR spectra of the S_{3D} paint (Figure 2A) show differences both in the sulfate asymmetric stretching (ν_1) and bending (ν_4) modes (see reference 14 for a detailed discussion of the vibrational features of the unaged paints): a decrement of the signal around 1050 cm^{-1} [$\nu_1(SO_4^{2-})$] and a change of the relative intensity between the bands at 620 and 597 cm^{-1} [$\nu_4(SO_4^{2-})$] are observed. According to literature,[19] these differences could reflect changes at the sulfate symmetry site and therefore of the $PbCr_{1-x}S_xO_4$ structure.

Figure 2B shows μ-ATR−mid-FTIR spectra in the organic binder's absorption region (2000−1250 cm^{-1}). For the aged paint S_{3D}, the formation of a broad and weak band, showing two maxima at ca. 1625 and 1575 cm^{-1}, is observed. In the same spectral region, the spectrum of aged sample A shows a much more intense band around 1575 cm^{-1}. At first glance, these signals could be ascribed to the asymmetric stretching COO^- band of metal-carboxylates formed as result of the interaction between the pigment (or its alteration products) and the drying oil's fatty acids.[20−22] However, since it is not possible to assign the observed bands to Pb(II) carboxylates,

dx.doi.org/10.1021/ac3021592 | Anal. Chem. 2013, 85, 860−867

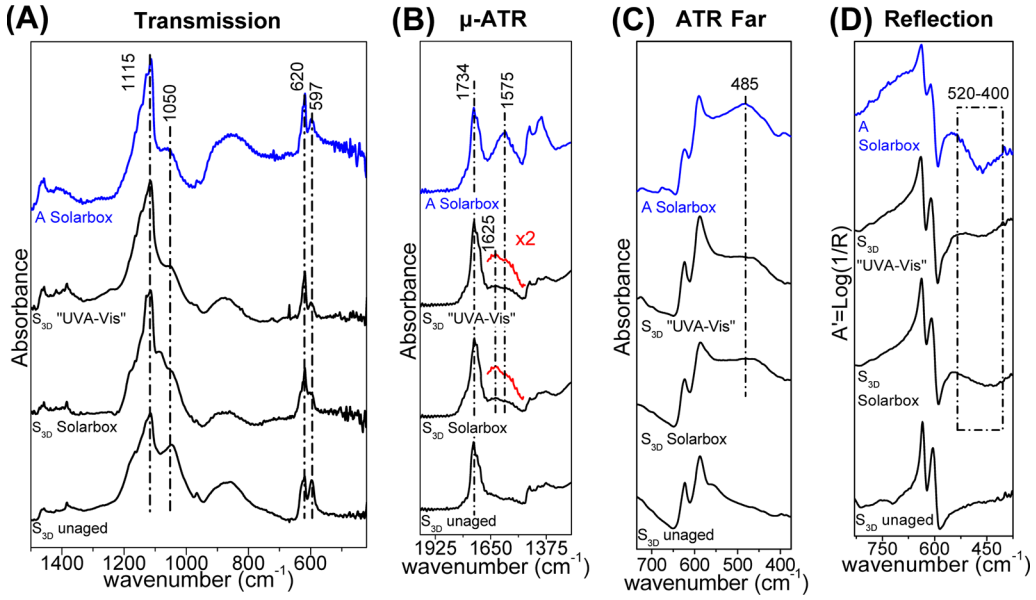

Figure 2. (A) Transmission mid-, (B) μ-ATR mid-, (C) ATR far-, and (D) reflection mid-FTIR spectra of (bottom to top) paint (black) S_{3D} before and after exposure to UVA-vis light and (blue) aged historic sample A. Solarbox and UVA-vis labels indicate the different systems for performing the aging treatments.

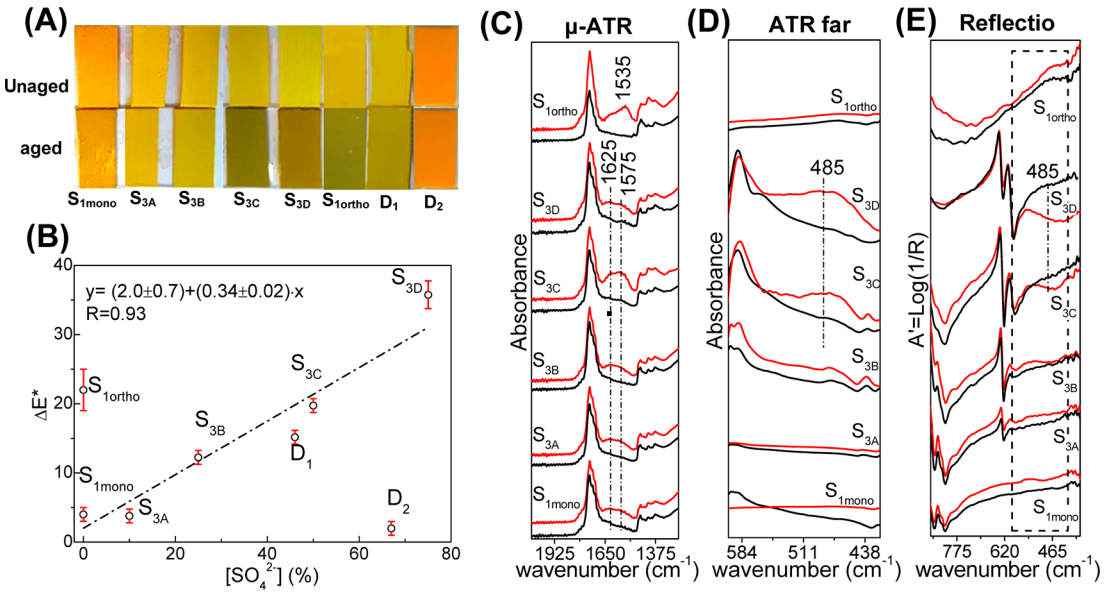

Figure 3. (A) Images and (B) changes of ΔE^* after exposure to the UVA-visible light of paint models containing different sulfate amounts. (B) The curve was calculated by linear fitting. (C) μ-ATR mid-, (D) ATR far-, and (E) reflection mid-FTIR spectra of paint models (bottom to top) S_{1mono}, S_{3A}, S_{3B}, S_{3C}, S_{3D}, and S_{1ortho}. In (E) the dotted rectangle indicates the energy range shown in (D).

whose asymmetric stretching COO^- band lies between 1510 and 1545 cm^{-1},[20−22] the origin of the bands observed for the aged chrome yellow-based models deserves further investigation.

ATR far-FTIR spectra of the aged samples (Figure 2C) show the formation of a new broad band around 485 cm^{-1}, attributable to the presence of amorphous Cr(III) oxides.[23] The same signal is visible in the spectral data acquired by portable reflection mid-FTIR (Figure 2D) in the form of an inverted band between 520 and 400 cm^{-1}. The higher sensitivity of reflection and ATR−FTIR spectroscopy for revealing compounds present as very thin superficial layers may explain why this band is not visible in the transmission mid-FTIR spectra.[24]

The limited thickness the alteration layer (ca. 2−3 μm) did not allow us to reveal significant differences before and after aging of the cross-sectional S_{3D} material by means of XRD and Raman investigations.

On the basis of these preliminary investigations, the orthorhombic $PbCr_{1-x}S_xO_4$ S_{3D} material shows a similar darkening behavior as the historic chrome yellow paint A. This phenomenon is not only induced by UVA-visible irradiation, but is already caused by blue light.

Characterization of Artificially Aged Paint Models Composed of Different Sulfate Amount. In Figure 3A, the visual aspect recorded from various paint models before and after the artificial aging (UVA-visible light, Solarbox, 800 h) are presented. The paints to which $BaSO_4$ or ZnS were added

dx.doi.org/10.1021/ac3021592 | Anal. Chem. 2013, 85, 860−867

(S_{1Ba}, S_{1Zn}, S_{3CBa}, and S_{3CZn}) showed features that are similar to their "parent" samples, S_{1mono} and S_{3C}, thus no data from these samples were included in Figure 3.

In all cases, a color change of the paint layer can be observed with the naked eye due to the aging; however, samples containing orthorhombic $PbSO_4$ or monoclinic lead chromate-based compounds (S_{1mono}, S_{3A}, S_{3B}, D_1, and D_2) did not reveal the same profound discoloration as did S_{3C} and S_{3D}, materials that contain orthorhombic $PbCr_{1-x}S_xO_4$ with sulfates exceeding 50%. Also, the paint made of orthorhombic $PbCrO_4$ (S_{1ortho}) shows a profound color change.

This observation was confirmed by UV−visible spectroscopy through the formation of a new band located at 530−620 nm, whose intensity increases with relative SO_4^{2-} abundance. These results (not shown in Figure 3) were expressed by a significant decrease of L^* and b^* values and by a slight or negligible decrease in a* value. As Figure 3B illustrates, a positive correlation between the ΔE^* values and the relative SO_4^{2-} abundance was revealed, with the exception of paints D_1, D_2, and S_{1ortho}. These results again indicate that it is not simply the amount of sulfate per se that strongly influences the susceptibility toward darkening, but more specifically the crystal form of the $PbCr_{1-x}S_xO_4$ co-precipitate (monoclinic or orthorhombic). In fact, a simple SO_4^{2-}-rich mixture of $PbSO_4$ and $PbCrO_4$ (D_2), where the $PbCrO_4$ remains present in monoclinic form, is not prone to discoloration, while the SO_4^{2-}-free orthorhombic $PbCrO_4$ (S_{1ortho}) appears unstable.

FTIR investigations carried out on the discolored paint S_{3C} (Figure 3, panels C−E) provided results similar to those obtained from S_{3D} and A. On the slightly discolored paints, S_{1mono}, S_{3A}, S_{3B}, D_1, and D_2, neither ATR far- nor reflection mid-FTIR analyses (Figure 3, panels D−E) showed any significant difference before and after the aging process (D_1 and D_2 spectral data are not shown in Figure 3).

μ-ATR mid-FTIR spectra (Figure 3C) reveal that both the profound and the slightly discolored paints show the presence of new signals at 1625 and 1575 cm^{-1}; only for the aged S_{1ortho}, this band is shifted to around 1535 cm^{-1}. In this latter case, an alteration reaction involving another process other than the Cr(VI) reduction to Cr(III) is possibly taking place. This is indirectly confirmed by ATR far- and reflection mid-FTIR measurements (Figure 3, panels D−E) that do not reveal the presence of the band around 485 cm^{-1}, indicative of the presence of amorphous Cr(III)-oxides.[23]

Because of the limited thickness (ca. 2−3 μm) of the alteration layer, neither XRD or Raman spectroscopy allowed us to reveal significant differences before and after aging of the aforementioned samples.

Cr and S K-edges XANES Investigations. *Unembedded Samples (Unfocused X-ray Beam Mode).* S and Cr K-edge XANES measurements were collected in unfocused mode from the surface of the unembedded paint models, both aged and unaged.

Cr K-edge spectra of several aged S_{3D} paint coupons and sample A (Figure 4A) showed a reduction of the original Cr(VI), as demonstrated by a decrease in the intensity of the Cr pre-edge peak at 5.993 keV (electronic transition s → 3d) and the absorption edge shift toward lower energies.[12] Also the post-edge features change, but it is difficult to interpret these on the basis of XANES data alone. Figure 4A shows that these changes are significant after the UVA-vis and UV light exposure. The decrease of the pre-edge peak intensity gradually progresses as a function of aging time (Figure 4A, compare

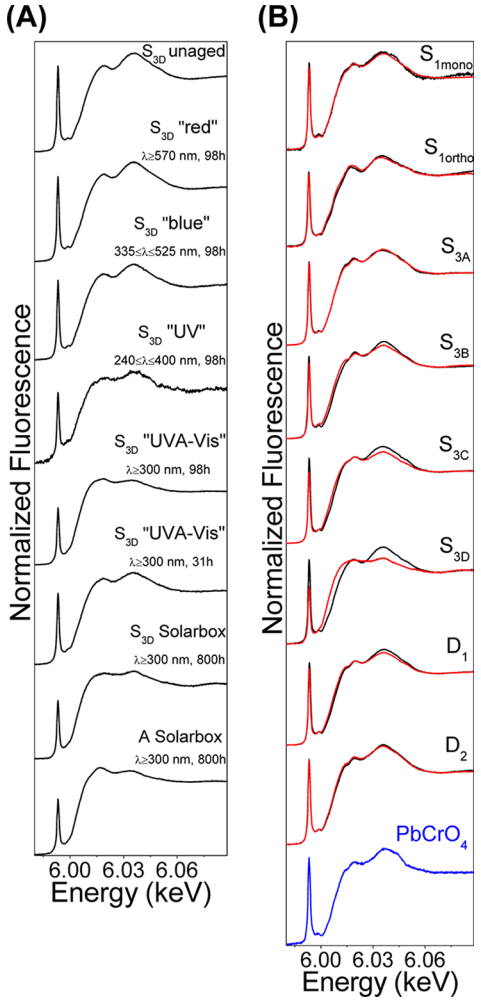

Figure 4. Cr K-edge XANES spectra (unfocused mode) of unembedded paints: (A) Aged sample A and S_{3D} paints, before and after irradiation by different wavelength bands. (B) (black) Unaged and (red) aged paint models containing different sulfate amounts. The spectrum of $PbCrO_4$ reference compound is shown in blue.

UVA-vis, $\lambda \geq 300$ nm, 31 h vs 98 h). While still minor differences were observed in the spectrum of the aged S_{3D} paint when employing the blue light, no change was visible upon irradiation of a S_{3D} coupon with red light. It follows that radiation containing wavelengths shorter than 525 nm is required to induce the Cr-reduction process.

In Figure 4B, Cr K-edge XANES spectra of aged and unaged paint models containing different sulfate amounts are intercompared (see also Figure S-3 of the Supporting Information for a magnification of the pre-edge peak region). Before aging (black line), all samples show spectra similar to that of the $PbCrO_4$ reference material (blue line), while after UVA-visible light exposure (red line), the Cr(VI) reduction becomes progressively more significant starting from a sulfate amount around 40% and an abundance of the orthorhombic phases >30 wt % . Before and after aging, the paints containing extra $BaSO_4$ or ZnS (S_{1Ba}, S_{1Zn}, S_{3CBa}, and S_{3CZn}, not shown in Figure 4B) revealed spectral features similar to those of S_{1mono} and S_{3C}, respectively.

Consistent with their slight discoloration, no significant differences were observed in the spectra of the aged paints containing the lowest amount of sulfate (S_{3A}), $PbCrO_4$ (S_{1mono} and S_{1ortho}), or in the case of mixture D_2. The brown-greenish

dx.doi.org/10.1021/ac3021592 | Anal. Chem. 2013, 85, 860−867

aspect of S_{1ortho} is not correlated to a clear modification of the Cr oxidation state. This lets us assume that other chemical reactions than just reduction cause the discolouration of this compound. Minor changes (decrement of the Cr K-pre-edge peak intensity of around 10%) were detected for the aged monoclinic paint S_{3B} (sulfate ca. 25 wt %) and D_1 (sulfate ca. 46 wt %).

These "bulk" XANES data are therefore consistent with the previously mentioned results obtained employing FTIR spectroscopy.

Regardless of the paint composition, S K-edge XANES spectra collected from paints A, S_{3A}-S_{3D}, and D_1 did not show any difference in the S oxidation state before and after aging, thus, results are not shown in Figure 4 (see reference 14 for XANES spectral features of the unaged samples). All S K-edge XANES spectra are characterized by a prominent peak at around 2.482 keV (electronic s → p transition), specific for the sulfate species,[5,25] while no indications of the presence of sulfide species (intense white line at 2.471 keV) were encountered.

Embedded Samples (Focused X-ray Beam Mode). Because of the relatively high penetration of the X-ray beam at the Cr K-edge energy (ca. 5 μm for lead chromate-based compounds), measurements in the unfocused mode did not allow us to obtain a reliable quantitative estimation of the amount of reduced Cr present in the thin alteration layer of paints. Thus, additional Cr K-edge XANES analyses were performed with a focused X-ray beam on cross sections of embedded paint models, S_{1mono}, S_{1ortho}, S_{3B}, S_{3C}, S_{3D}, and D_1, aged by UVA-visible light. Series of XANES spectra were collected along a line perpendicular to the exposed surface of these samples, employing a step size between 0.5 and 2 μm.

All spectra of the sulfate-poor samples, S_{1mono}, S_{1ortho}, S_{3B}, and D_1, are very similar to those obtained from the corresponding unaged paints and are therefore not shown in Figure 5. As observed for the historic paint A, measurements performed on S_{3C} and S_{3D} (Figure 5A and Figure S-4A of the Supporting Information for all spectra) show a significant difference between the brownish surface and the yellow layer below.

The data recorded from S_{1mono}, S_{1ortho}, S_{3B}, and D_1 can be adequately fitted when the XANES spectra of $PbCrO_4$ and either viridian ($Cr_2O_3{\cdot}2H_2O$) or Cr(III) acetate [$Cr(Ac)_3$] are included in the fitting model. For S_{3C} and S_{3D}, similar to sample A,[12] three fitting components, such as $PbCrO_4$, $Cr_2O_3{\cdot}2H_2O$, and either Cr(III) potassium sulfate dodecahydrate [$KCr(SO_4)_2{\cdot}12H_2O$] or Cr(III) acetylacetonate [$Cr(acac)_3$] were necessary to obtain a good description of the spectra recorded along the discolored first 2−3 μm of the cross section (see Figure S-4B of the Supporting Information for an example). As before, only two components [$PbCrO_4$ and $Cr_2O_3{\cdot}2H_2O$/$Cr(Ac)_3$] are necessary to fit the spectra recorded at greater depth. The assumption that $KCr(SO_4)_2{\cdot}12H_2O$ may be present is reasonable since sulfate species are part of the crystalline structure of the pigment itself, while potassium can be present as an impurity (K_2CrO_4 and K_2SO_4 were used as starting reagents for the powders' synthesis). In view of the similarities between the XANES spectra of the $KCr(SO_4)_2{\cdot}12H_2O$, $Cr(acac)_3$, and $Cr(Ac)_3$ reference compounds,[12] both fitting models yield approximately the same Cr(VI):Cr(III) ratio percentage.

For the aged samples S_{1mono}, S_{1ortho}, S_{3B}, and D_1, the relative Cr(VI) concentration, expressed as $[Cr(VI)]/[Cr_{total}]$, was estimated to be around 70−80% along the first 3 μm of the cross section, while for S_{3C} and S_{3D} (Figure 5B), this value progressively increased from the superficial brown layer (ca. 40−60%) toward the yellow bulk of the sample (ca. 60−80%). An overview of all these values is reported in Table S-1 of the Supporting Information.

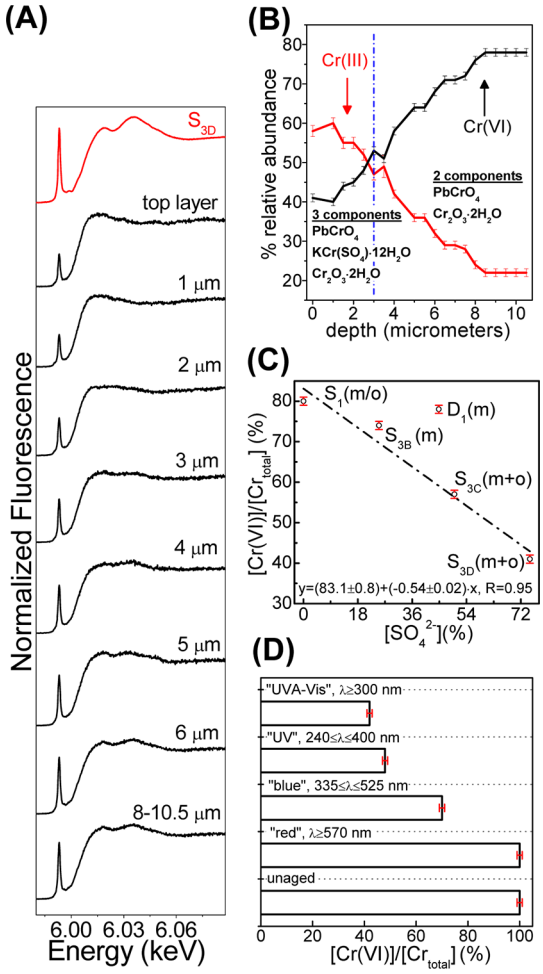

Figure 5. (A) Series of Cr K-edge XANES spectra recorded from cross-sectioned paint S_{3D}: (red) before and (black) after UVA-visible light exposure. (B) Quantitative estimation of (black) Cr(VI) and (red) Cr(III) relative abundance percentages vs the depth obtained by linear combination fitting of spectra shown in (A) [see also Figure S-4 of the Supporting Information]. (C) The Cr(VI) relative abundance percentage present at the aged exposed surface vs the sulfate amount and (D) as a function of the wavelength bands employed to irradiate several S_{3D} paints. In (C) "m" and "o" indicate monoclinic and orthorhombic phases.

The fitting of XANES spectra from aged paints (Figure 5C) reveals that the amount of the original Cr(VI) at the surface exposed to aging progressively decreases going from S_{1mono}/S_{1ortho} (0% sulfate) to S_{3D} (sulfate ca. 75 wt %). Similarly, the Cr(VI) at the surface of aged S_{3D} coupons depends strongly on the wavelength range employed for the aging (Figure 5D): when exposed to red light, 100% of Cr(VI) remains, while in the case of UV and UVA-vis radiation, only ca. 40−50% of the superficial Cr(VI) is left.

These results confirm in a semiquantitative and surface-specific way the qualitative findings obtained by UV−visible spectroscopy (Figures 1C and 3B).

The formation of a Cr(III)-rich brown alteration layer resulting from photochemical treatment of S_{3D} and A is similar

dx.doi.org/10.1021/ac3021592 | Anal. Chem. 2013, 85, 860−867

to that observed in previous works.[26,27] In these studies, by employing a high relative humidity condition and the presence of SO_2, the color alteration of zinc yellow paints ($K_2O{\cdot}4ZnCrO_4{\cdot}3H_2O$) was demonstrated to be attributable to the formation of Cr(III) and dichromate species. However, in contrast to their conclusions, the present XANES data do not reveal any indications about the presence of dichromate compounds: fits of reduced quality were obtained, when in the model, this class of Cr(VI)-based compounds was included.

CONCLUSION

In this paper, the combined use of UV−visible diffuse reflectance, FTIR, and SR μ-XANES spectroscopy allowed us to characterize the wavelength range of the UV−vis spectrum that drives forward the degradation of the different types of chrome yellow pigments and to experimentally confirm the key role that sulfate anions are playing. We demonstrated that the degradation of sulfur-rich $PbCr_{1-x}S_xO_4$ solid solutions requires irradiation with either UVA-visible, UV, or blue light, while red light, with an energy per photon smaller than the absorption energy of $PbCrO_4$, is insufficiently energetic to trigger the reaction. To avoid photoinduced darkening of the susceptible variants of the lead chromate-based pigments, it is advisible to minimize their exposure to light with wavelengths shorter than about 525 nm.

Under suitable photochemical irradiation, $PbCr_{1-x}S_xO_4$ containing less than 50% sulfates are most likely to crystallize in the stable monoclinic form and show a reduced tendency toward darkening and reduction. The chrome yellow co-precipitates richer in sulfates (≥50%) are mostly formed in the orthorhombic form and have a relatively high susceptibility toward browning.

We suspect that these observations can be partially attributed to the higher solubility of the $PbCrO_4$ and $PbCr_{1-x}S_xO_4$ orthorhombic forms than their monoclinic equivalents and thus to the higher availability of chromate ions for redox reactions.

No effects on the alteration of lead chromate-based compounds were observed when sulfate and sulfide species were not included in the crystalline structure.

μ-XANES analyses performed on aged model paints revealed the presence of the highest relative Cr(III) concentration at the exposed discolored surface (thickness around 2−3 μm). In particular, its abundance gradually increases when going from either pure $PbCrO_4$ or SO_4^{2-}-poor aged samples (around 20%) to that containing the highest sulfate amount (up to ca. 60%). The discoloration of the S_{1ortho} material appears to be a consequence of another mechanism, not attributable to a reduction of the original Cr(VI).

Part 5 will focus on the local S and Cr speciation in microsamples from paintings by Van Gogh and contemporaries and how the local SO_4^{2-} abundance and the crystal form of the lead chromate-based yellow is correlated to the reduction behavior. The fact that in the original microsamples investigated up to now, reduced Cr(III) is more frequently observed in those areas where the chrome yellow is in contact with (degraded) varnish layers suggests a possible role of organic components (e.g., as redox partners for chromate ions) and the structure and permeability of the cover layers. With the aim of exploring how the speed of degradation of chrome yellow might be influenced by the nature of the organic binder in the paint, investigations of additional model samples prepared by mixing different binders and different lead chromate-based compounds are ongoing.

ASSOCIATED CONTENT

Supporting Information

Additional information as noted in text. This material is available free of charge via the Internet at http://pubs.acs.org.

AUTHOR INFORMATION

Corresponding Author

*E-mail: koen.janssens@ua.ac.be. Tel: +32 3 265 33 22. Fax: +32 3 265 32 33.

Notes

The authors declare no competing financial interest.

ACKNOWLEDGMENTS

This research was supported by grants from ESRF (experiment EC-799), the Interuniversity Attraction Poles Programme-Belgian Science Policy (IUAP VI/16), and the BELSPO-SDD S2-ART (SD/RI/04) project. The text also presents results from GOA "XANES meets ELNES" (Research Fund University of Antwerp, Belgium) and FWO (Brussels, Belgium) projects G.0704.08 and G.01769.09. The EU FP7 programme CHARISMA (Grant Agreement 228330) and MIUR (PRIN08, *Materiali e sistemi innovativi per la conservazione dell'arte contemporanea* 2008 FFXXN9) are also acknowledged.

REFERENCES

(1) Townsend, J. H. *Stud. Conserv.* **1993**, *38*, 231−254.
(2) Dredge, P.; Wuhrer, R.; Phillips, M. R. *Microsc. Microanal.* **2003**, *9*, 139−143.
(3) Favaro, M; Bianchin, S.; Pietro, A.; Vigato, P.A.; Vervat, M. *J. Cult. Herit.* **2010**, *11*, 265−278.
(4) Correia, A. M.; Oliveira, M. J. V.; Clark, R. J. H.; Ribeiro, M. I.; Duarte, M. L. *Anal. Chem.* **2008**, *80*, 1482−1492.
(5) Cotte, M.; Susini, J.; Metrich, N.; Moscato, A.; Gratziu, C.; Bertagnini, A.; Pagano, M. *Anal. Chem.* **2006**, *78*, 7484−7492.
(6) Radepont, M.; de Nolf, W.; Janssens, K.; Van der Snickt, G.; Coquinot, Y.; Klaassen, L.; Cotte, M. *J. Anal. At. Spectrom.* **2011**, *26*, 959−968.
(7) Samain, L; Silversmit, G.; Sanyova, J.; Vekemans, B.; Salomon, H.; Gilbert, B.; Grandjean, F.; Long, G. J.; Hermann, R. P.; Vincze, L.; Strivay, D. *J. Anal. At. Spectrom.* **2011**, *26* (5), 930−94.
(8) Robinet, L.; Spring, M.; Pagès-Camagna, S.; Vantelon, D.; Trcera, N. *Anal. Chem.* **2011**, *83*, 5145−5152.
(9) Van der Snickt, G.; Dik, J.; Cotte, M.; Janssens, K.; Jaroszewicz, J.; De Nolf, W.; Groenewegen, J.; Van der Loeff, L. *Anal. Chem.* **2009**, *81* (7), 2600−2610.
(10) Van der Snickt, G.; Janssens, K.; Dik, J.; De Nolf, W.; Vanmeert, F.; Jaroszewicz, J.; Cotte, M.; Falkenberg, G.; Van der Loeff, L. *Anal. Chem.* **2012**, DOI: 10.1021/ac3015627.
(11) Miliani, C.; Rosi, F.; Brunetti, B. G.; Sgamellotti, A. *Acc. Chem. Res.* **2010**, *43*, 728−738.
(12) Monico, L.; Van der Snickt, G.; Janssens, K.; De Nolf, W.; Miliani, C.; Verbeeck, J.; Tian, H.; Tan, H.; Dik, J.; Radepont, M.; Cotte, M. *Anal. Chem.* **2011**, *83*, 1214−1223 and references therein.
(13) Monico, L.; Van der Snickt, G.; Janssens, K.; De Nolf, W.; Miliani, C.; Dik, J.; Radepont, M.; Hendriks, E.; Geldof, M.; Cotte, M. *Anal. Chem.* **2011**, *83*, 1224−1231 and references therein.
(14) Monico, L.; Janssens, K.; Miliani, C.; Brunetti, B. G.; Vagnini, M.; Vanmeert F.; Falkenberg, G.; Abakumov, A.; Lu, Y.; Tian, H.; Verbeeck, J.; Radepont, M.; Cotte, M.; Hendriks, E.; Geldof, M.; van der Loeff, L.; Salvant, J.; Menu, M. *Anal. Chem.* 2012, 10:1021/ac302158b and references therein.
(15) Clementi, C.; Miliani, C.; Romani, A.; Favaro, G. *Spectrochim. Acta, Part A* **2006**, *64*, 906−912.

(16) Solé, V. A.; Papillon, E.; Cotte, M.; Walter, P.; Susini, J. *Spectrochim. Acta, Part B* **2007**, *62*, 63−68.
(17) Ravel, B.; Newville, M. *J. Synchrotron Radiat.* **2005**, *12*, 537−541.
(18) Cole, R. J. *The Research Association of British Paint, Colour and Varnish Manufacturers* **1955**, *10* (14), 1−62.
(19) Stoilova, D.; Georgiev, M.; Marinova, D. *J. Mol. Struct.* **2005**, *738*, 211−215.
(20) Robinet, L.; Corbeil, M. C. *Stud. Conserv.* **2003**, *48*, 23−40.
(21) Cotte, M.; Checroun, E.; Susini, J.; Dumas, P; Tchoreloff, P.; Besnard, M.; Walter, Ph. *Talanta* **2006**, *70*, 1136−1142.
(22) Cotte, M.; Checroun, E.; Susini, J.; Walter, P. *App. Phys. A: Mater. Sci. Process.* **2007**, *89*, 841−848.
(23) Musić, S.; Malijković, M.; Popović, S. *Croatia Chemica Acta* **1999**, *72*, 789−802.
(24) Ricci, C.; Miliani, C.; Brunetti, B. G.; Sgamellotti, A. *Talanta* **2006**, *69*, 1221−1226.
(25) Vairavamurthy, A. *Spectrochim. Acta, Part A* **1998**, *54*, 2009−2017.
(26) Casadio, F.; Xie, S.; Rukes, S. C.; Myers, B.; Gray, K. A.; Warta, R.; Fiedler, I. *Anal. Bioanal. Chem.* **2011**, *399*, 2909−2920.
(27) Zanella, L.; Casadio, F.; Gray, K. A.; Warta, R.; Ma, Q.; Gaillard, J.-F. *J. Anal. At. Spectrom.* **2011**, *26*, 1090−1097.